

Characterization of Composite Structure Surface Uniformity using Interval Based Gradient Field Histogram Analysis of Thermographic Images (IGF-HA)

Mahmoud Zaki Iskandarani

Department of Electronics and Communications Engineering, Faculty of Engineering,
Al-Ahliyya Amman University, Salt-Jordan

Article history

Received: 22-04-2018

Revised: 09-05-2018

Accepted: 22-05-2018

Email: m.iskandarani@ammanu.edu.jo

Abstract: This paper presents a new approach to composite surface characterization using Image Histogram Analysis as a function of Gradient Field. Image sequences are weighed and combined in order to present a pattern change in the thermal response of a tested composite structure. Reaction Injection Molding samples used and subjected to thermal energy to characterize their surface uniformity and any existing damage. A threshold value is used for the purpose of segmenting and separating damaged from undamaged areas in the tested composite structure. Gradient field analysis established the critical time at which the surface started to show damage and segmented the tested images into areas of concern. The resulting histograms cover four main regions of interest according to the gradient intensities as a function of time. Each region is divided into eight subsections according to the corresponding limit value, resulting in thirty two subsections. Correlation between region gradient field and its histogram resulted in uncovering of surface deformities as a function of surface area thermal storage. The process is modeled mathematically.

Keywords: Histogram Equalization, Histogram Specification, Gradient Norm, Edge Detection, Gray Level Mapping, Information Entropy, Segmentation

Introduction

Image enhancement focuses on reducing image noise, removing artifacts and preserving details. Its purpose is to highlight certain image features for analysis, diagnosis, characterization and decision making. Histogram and Gradient analysis plays a crucial role in image processing applications for the purpose of better image visualization and details enhancements in order to achieve objectives such as segmentation and edge detection (Suganya *et al.*, 2013; Zhou and Yicong, 2016; He Wen and Li, 2016; Cheolkon and Yang, 2016; Qiong *et al.*, 2016).

Edge detection is popular technique used in digital image processing. The process comprises identifying and locating sharp discontinuities in an image. The boundaries of object surfaces discontinuities characterize boundaries of objects in an object. Edges in an image are a result of sudden change of multiple characteristics at pixel level. Such changes are observed as a function of color, texture, shade or light absorption (Huang *et al.*, 2013; Nikolova *et al.*, 2013;

Nikolova and Steidl, 2014; Faridul *et al.*, 2016; Peng *et al.*, 2015). These characteristics enable estimating the size, orientation, depth and surface features in an image.

Histogram Analysis (HA) and Histogram Equalization (HE) algorithm is a known image enhancement algorithm. It affects the gray levels of an image according to the Probability Distribution Function (PDF) and Cumulative Distribution Function (CDF) of the image and expands the dynamic range of the gray level distribution to enable better visualization and provide important statistical analysis.

HE assigns the intensity values of pixels in the input image such that the output image contains a uniform distribution of intensities. It alters the image contrast to obtain a uniform histogram. This technique can be used on different parts of an image. The HE technique usually increases the overall contrast of any image, depending on how close the image pixel values. Through this adjustment, the intensities can be distributed on the histogram as a function of the input intensities and the applied transformation function.

HE accomplishes its task by spreading out the most frequent intensity values. The method is useful in images with backgrounds and foregrounds that are both bright or both dark. In particular, the method can lead to better visualization of structures.

Composites are now extensively being used for structural support. The overall properties of the composites are superior to those of the individual constituents. Advantages of composites over their conventional counterparts are the ability to meet diverse design requirements with significant weight savings as well as strength-to-weight ratio. Composite properties (e.g. stiffness, thermal expansion etc.) can be varied continuously over a broad range of values under the control of the designer. Common fiber reinforced composites are composed of fibers and a matrix. Fibers are the reinforcement and the main source of strength while matrix glues all the fibers together in shape and transfers stresses between the reinforcing fibers. The fibers carry the loads along their longitudinal directions. Sometimes, filler might be added to smooth the manufacturing process, impact special properties to the composites. Due to this, it is essential to illustrate and record the properties of these composites. The property of the fiber depends on its structure, changes in the morphology of fibre before and after the composite is subjected to external factors. Therefore it is important to have and analyze images of composites to establish their structural health and fitness for function (Usmantiagar *et al.*, 2013; Ma and Liu, 2016; Wang *et al.*, 2016; Liang *et al.*, 2016; Ashwini and Yuvaraju, 2016; Iskandarani, 2017).

Object appearance and shape can often be characterized by the distribution of intensity gradients or edge directions using Gradient Analysis (GA) without the need for accurate data regarding edge positions. Gradient strengths vary over a wide range owing to local variations in illumination and foreground-background contrast, so effective local contrast normalization turns out to be essential for good performance. The main objective in this feature extraction stage is to capture the shape of some structures. Local shape information can be described through gradient intensity and orientations. Histograms of gradients basically provide information about the occurrence of gradient orientations in a localized region of the images. Hence, they are able to characterize shapes in regions of concern (Santhi and Wahida Banu, 2015; Randa and Rabab Farouk, 2015; Lidong *et al.*, 2015; Honglie *et al.*, 2015; Kuldeep *et al.*, 2015; Xiangzhi, 2015; Wenda *et al.*, 2014; Jing and Nor Ashidi, 2014; Mohammad Farhan *et al.*, 2014b; 2014a; Kuldeep and Rajiv, 2014a; Chien-Cheng *et al.*, 2014).

In this work, the process is applied to the thermally pulsed composite structure output images over periods of time, obtaining histograms of gradient directions or edge orientations over the pixels of each image. The use of gradient distribution specification intensity histogram for

composite structure surface characterization is proposed instead of intensity histogram, which is proved previously to be invariant across many different types of images.

Materials and Methods

Reaction Injection Molding (RIM) composite components, which represents an enhanced type of fiberglass composite structures that can be tailored to meet the need of a specific application are shaped into rectangles (130×150 mm). Images obtained for all tested components pre and post impact using PVT technique. HA and GA analysis techniques are employed for feature extraction and characterization.

The resulting feature maps for tested samples are used to derive mathematical expression governing the behavior of the tested components under PVT. The resulting maps encoded into arrays of data to correlate Thermal Flow features with HA and GA features. The reference encoding feature map is shown in Fig. 1.

For Pulse Video Thermography (PVT) the equipment used consisted of heat source and thermal imaging system. The heat source is adequately fast pulse. Pulse obtained by discharging several Kilojoules of energy through each of two Xenon flash tubes, which are directed at the component under test. The thermal imaging part of the experiment was carried out using an advanced thermal camera. Each thermal event was recorded directly on a specific storage.

The main objective is to realize image segmentation through edge detection to obtain region growing and intensity information in order to detect structural irregularities. The used process comprised the following:

- Acquisition of a thermal image
- Conversion to Grey
- Histogram Generation
- Histogram Generation of Gradient Fields

a_1, b_1	a_1, b_2				a_1, b_n
a_m, b_1	a_m, b_2				a_m, b_m

Fig. 1: Encoding reference map

Results

Figure 2-5 show histogram mapping for a composite component subjected to thermal pulse with images taken over period of time to monitor thermal propagation and sample surface uniformity. The intervals are taken 5 minutes apart with the time interval between the first and

second sampling point is 9 min as it took time for the sample to start discharging its thermally stored energy and hence to see any irregularities on the surface of within the structure. Figure 6-9 show histogram mapping for associated gradient fields, presenting the main gradient components of sampled thermal images.

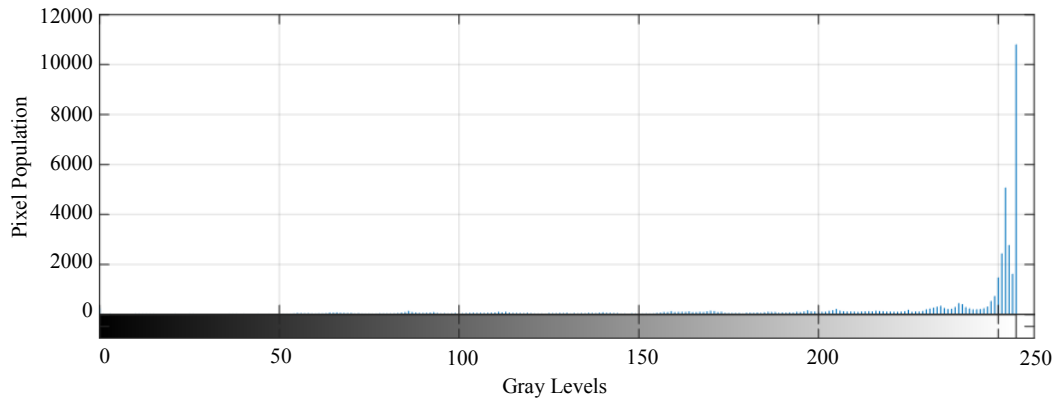


Fig. 2: Histogram of a PVT image after 5 min

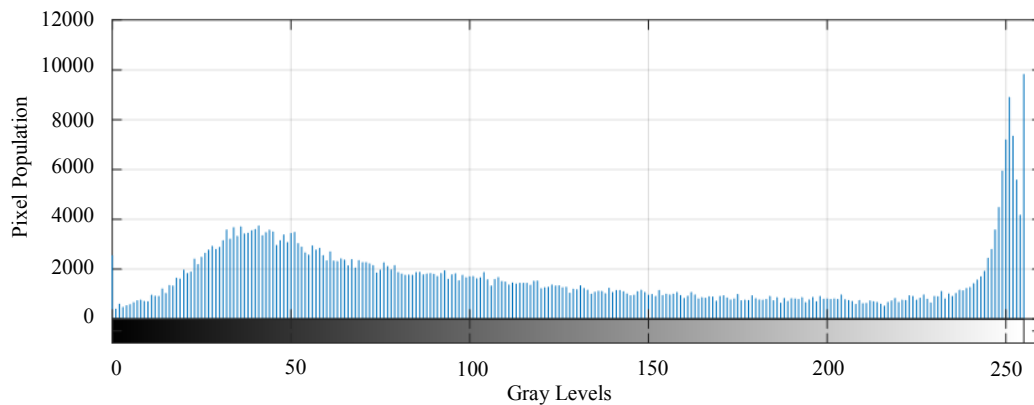


Fig. 3: Histogram of a PVT image after 14 min

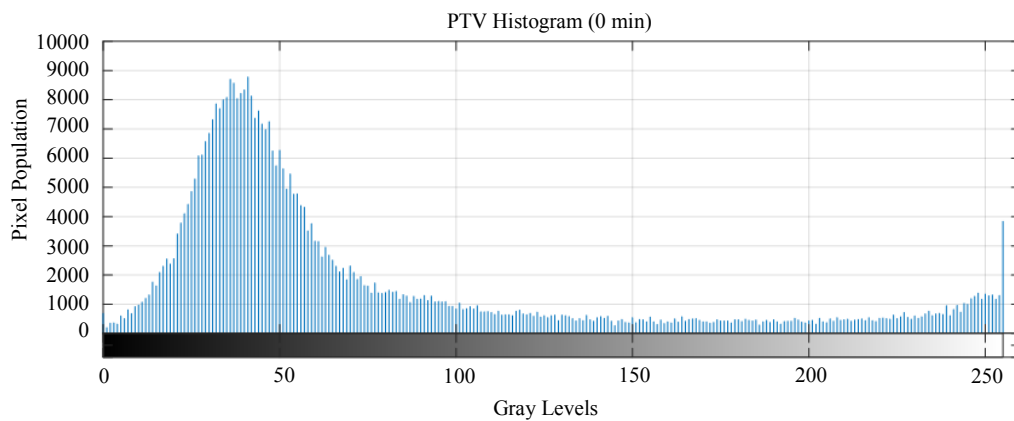


Fig. 4: Histogram of a PVT image after 19 min

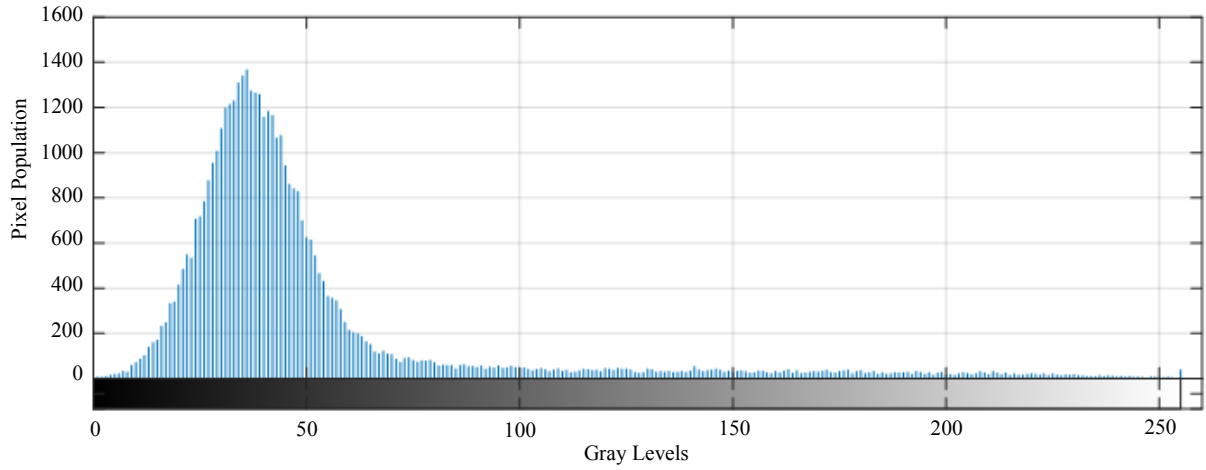


Fig. 5: Histogram of a PVT image after 24 min

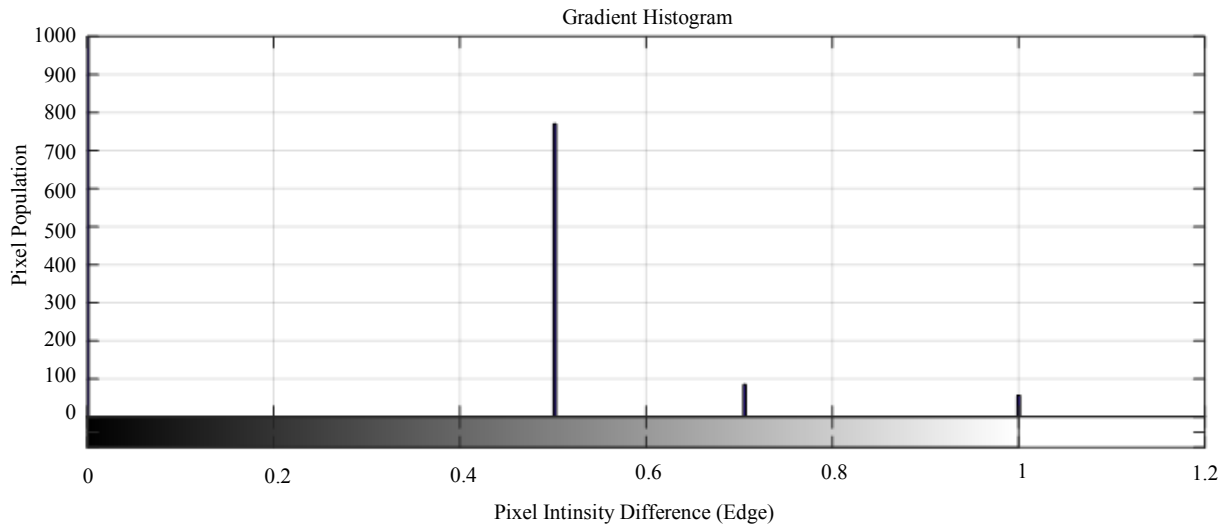


Fig. 6: Histogram of gradient of PVT image after 5 min

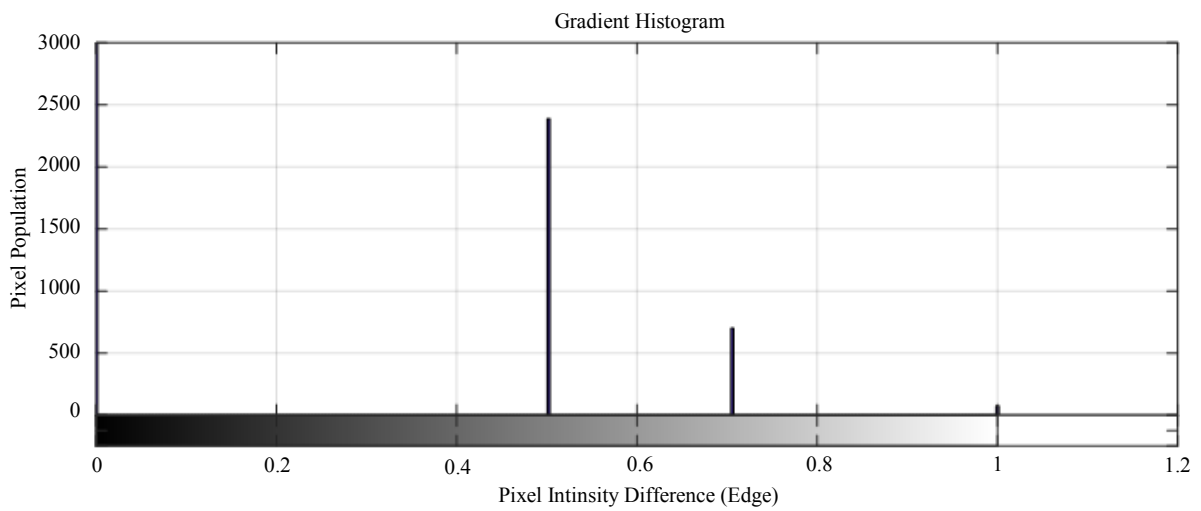


Fig. 7: Histogram of gradient of PVT image after 14 min

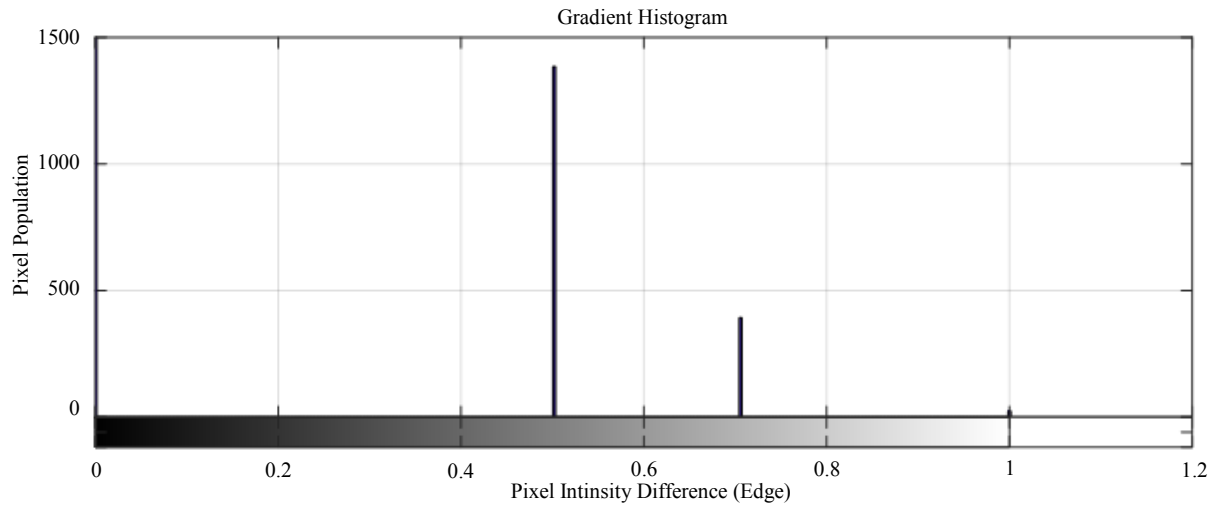


Fig. 8: Histogram of gradient of PVT image after 19 min

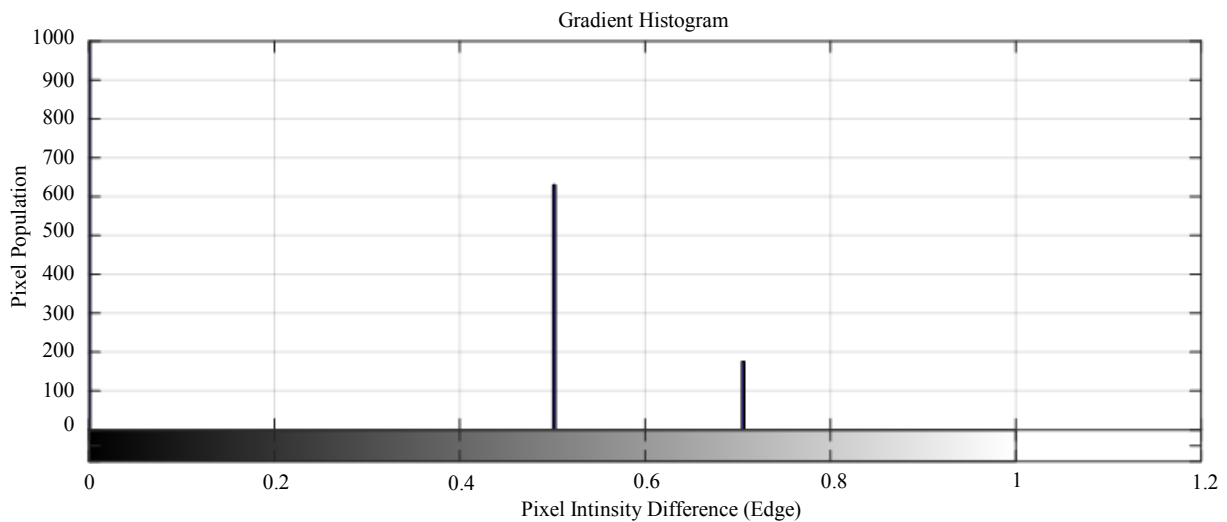


Fig. 9: Histogram of gradient of PVT image after 24 min

Analysis and Discussion

Figure 10-17 show the detailed octet analysis of the time dependent thermal response of a composite structure. By analyzing the plots and cross-correlating the detailed thermal responses with gradient histograms, the results indicated that the critical time response that proves the presence of surface non-uniformity and /or surface damage is 14 min. At 14 min, an apparent segmentation and edge started to appear between the left and right sides of the sample due to thermal storage. This is proved through the accumulative array values in Table 1, where an edge is recorded at 14 min for arrays 3 through to 6, while surrounded by two arrays of increasing and two arrays of decreasing pixel populations. This is significant evidence that proves that the component has a problem

such as damaged fiber-matrix and/or fiber-matrix density variation.

In addition and by cross-correlation between the analyzed histogram data and the gradient data in Fig. 6 to 9 and Table 2, segmentation is confirmed; whereby a gradient amplitude redistribution occurs, forming edges at $t = 14$, indicating the existence of two main thermally charged regions.

The results show modeling the dynamic response of the tested composite structure of the mentioned type as capacitive circuits with four main testing time points:

1. $t = 5$ min
2. $t = 14$ min
3. $t = 19$ min
4. $t = 24$ min

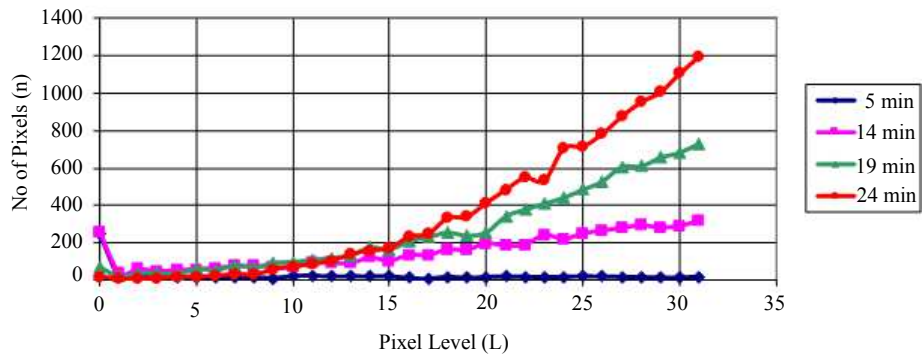


Fig. 10: Array 1 pixel distribution analysis

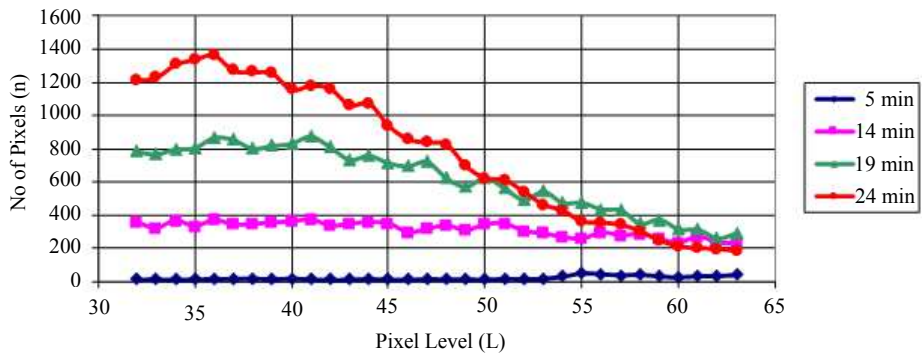


Fig. 11: Array 2 pixel distribution analysis

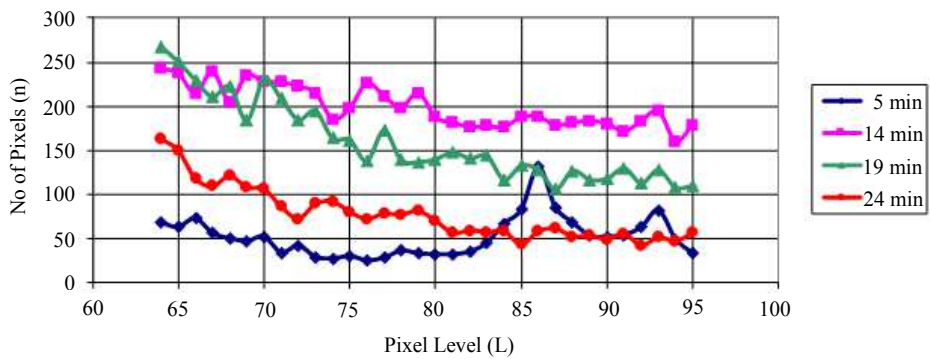


Fig. 12: Array 3 pixel distribution analysis

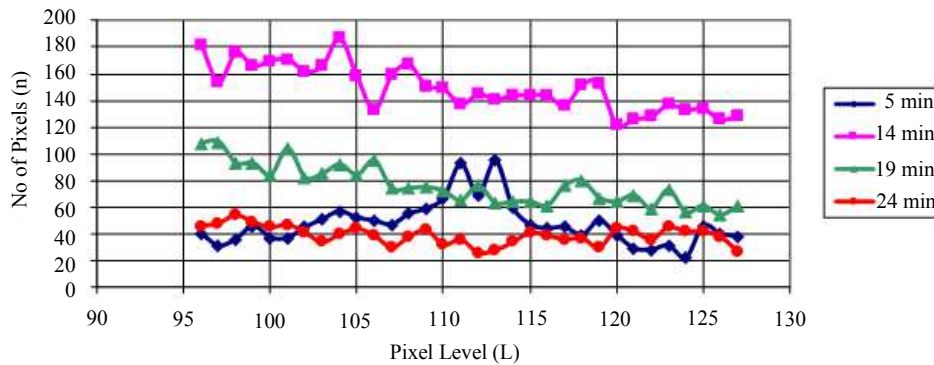


Fig. 13: Array 4 pixel distribution analysis

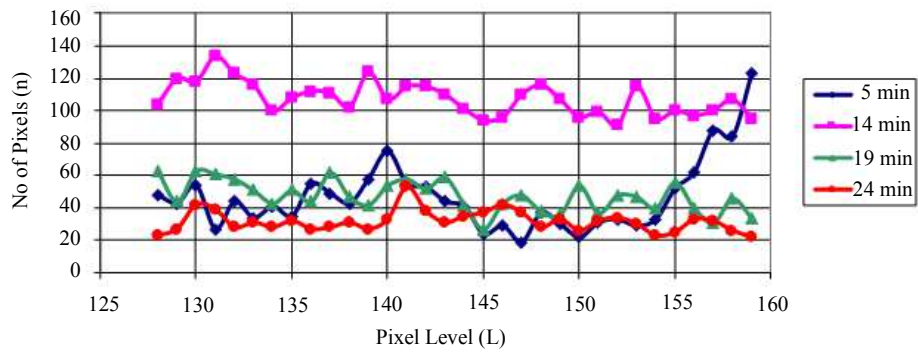


Fig. 14: Array 5 pixel distribution analysis

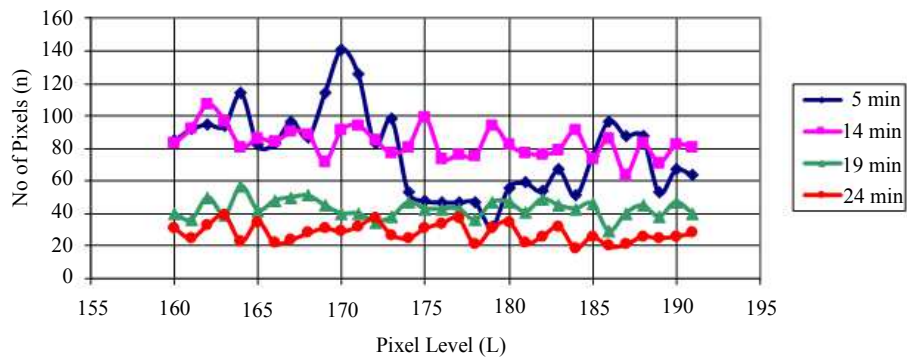


Fig. 15: Array 6 pixel distribution analysis

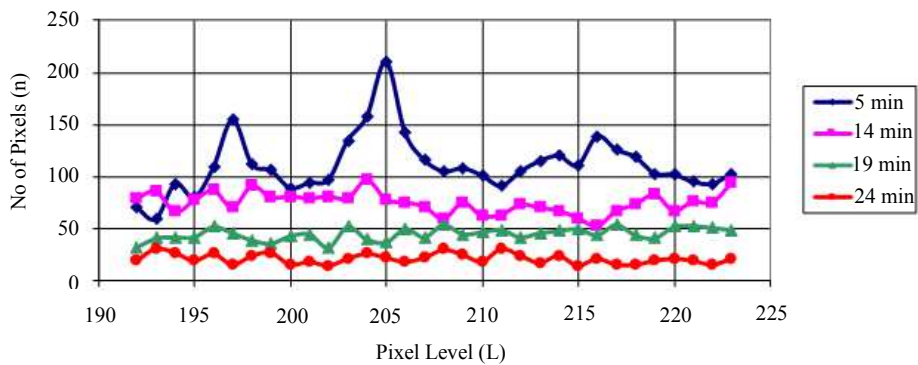


Fig. 16: Array 7 pixel distribution analysis

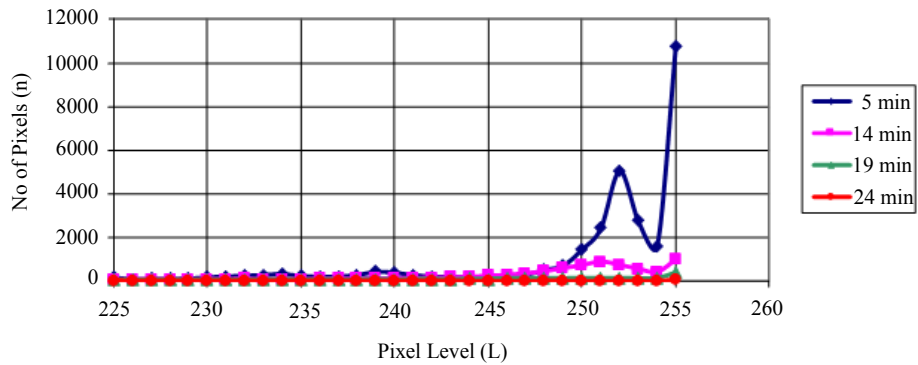


Fig. 17: Array 8 pixel distribution analysis

Table 1: Array-Pixel distribution as function of time

Array	5 min	14 min	19 min	24 min
1	800	4960	8406	11404
2	792	10054	19851	25155
3	1657	6375	5108	2469
4	1525	4781	2437	1253
5	1495	3438	1519	1013
6	2484	2673	1380	901
7	3562	2393	1440	673
8	30885	8526	3059	332

Table 2: Edge detection using gradient field data

G ray level	Value at t = 5	Value at t = 14	Value at t = 19	Value at t = 24
0	13488	11234	12600	13594
128	770	2389	1384	630
180	85	701	392	176
255	57	76	24	0

Two main effects realized:

1. Thermal capacitive storage within the tested component
2. segmentation and region forming (at 14 min) due to non-uniform composite structure and presence of damage within fiber-matrix system

This leads to the formation of capacitive areas charging-discharging in parallel and feeding each other, until all of the regions finally come to balance, with two separated regions representing two thermally capacitive sources that will start to discharge through the component over a period of time T .

Equation 1 describes the overall behavior of pixel distribution as a function of capacitive regions:

$$P_{Total} = \sum_{j=1}^Q P_{region j} \quad (1)$$

Each region can be described by sub-arrays of pixel distribution as presented in Equation 2:

$$P_{Total} = \sum_{k=1}^L \sum_{j=1}^Q P_{(Array_k)region j} \quad (2)$$

Where:

- L : Number of arrays containing gray level intensities and in this case, we have 8 arrays each comprising of 32 levels, giving 256 grey levels
- Q : Number of capacitive regions formed upon testing within the composite structure and in this case two main segmented regions observed at $t = 14$ minutes and totally separated at $t = 19$ min

Until total charge or total discharge of thermal energy, each region will suffer dynamic and time related

change in pixel population, which affects the expression in Equation 1 and results in Equation 3:

$$P_{Total} = \sum_{j=1}^Q \left(\frac{\Delta P_{region j}}{\Delta t} \right) p(t)_{region j} \quad (3)$$

From Equation 1, Equation 3 becomes:

$$P_{Total} = \sum_{k=1}^L \sum_{j=1}^Q \left(\frac{\Delta P_{(Array_k)region j}}{\Delta t} \right) p(t)_{(Array_k)region j} \quad (4)$$

Using Equations 1 to 4 and obtained data, the following matrix is realized:

$$p(t)_{(Array_k)region j} = \begin{bmatrix} P_{1,1} & P_{1,2} & P_{1,3} & P_{1,4} \\ P_{2,1} & P_{2,2} & P_{2,3} & P_{2,4} \\ P_{3,1} & P_{3,2} & P_{3,3} & P_{3,4} \\ P_{4,1} & P_{4,2} & P_{4,3} & P_{4,4} \\ P_{5,1} & P_{5,2} & P_{5,3} & P_{5,4} \\ P_{6,1} & P_{6,2} & P_{6,3} & P_{6,4} \\ P_{7,1} & P_{7,2} & P_{7,3} & P_{7,4} \\ P_{8,1} & P_{8,2} & P_{8,3} & P_{8,4} \end{bmatrix} \quad (5)$$

where, $P_{n,m}$: pixel distribution in Array n, region m

Substituting the collected data values, normalizing by dividing with data values at $t = 14$ min, leads to the Expression in 6:

$$p(t_{Seg})_{(Array_k)region j} = \begin{bmatrix} 0.26 & 1.00 & 0.80 & 0.39 \\ 0.32 & 1.00 & 0.51 & 0.26 \\ 0.44 & 1.00 & 0.44 & 0.30 \\ 0.93 & 1.00 & 0.52 & 0.34 \end{bmatrix} \quad (6)$$

The values in 6 can be approximated and the segmentation band narrowed as shown in 7:

$$P(t_{Seg})_{(Array_k)region_j} = \begin{bmatrix} 0.30 & 1.00 & 0.80 & 0.40 \\ 0.30 & 1.00 & 0.50 & 0.30 \\ 0.40 & 1.00 & 0.40 & 0.30 \end{bmatrix} \quad (7)$$

Removing the edge factors at $t = 14$ min results in the characterization matrix for the type and composition of the tested structure as given in Expression 8:

$$P_{(14min)characterization} = \begin{bmatrix} 0.30 & 0.80 & 0.40 \\ 0.30 & 0.50 & 0.30 \\ 0.40 & 0.40 & 0.30 \end{bmatrix} \quad (8)$$

Removing the factors at $t = 19$ min at which time total separation of regions occurs results in Expression 9:

$$P_{(19min)characterization} = \begin{bmatrix} 0.30 & 1.00 & 0.40 \\ 0.30 & 1.00 & 0.30 \\ 0.40 & 1.00 & 0.30 \end{bmatrix} \quad (9)$$

The noted values and realized symmetry along both diagonals and middle line is clear. It is a function of fiber matrix structure and indicates the presence of thermal storage areas, which points towards the existence of structural deformation.

Conclusion

The new technique is an excellent beginning to correlate both histogram analysis and gradient fields to uncover problems within composite structures. Using Pulse Video Thermography and such techniques will lead to a reliable Non-Destructive Technique that can be applied across a wide range of industries, starting with automotive and ending with aerospace.

Ethics

There are no ethical issues with this article.

References

Ashwini, B. and B. Yuvaraju, 2016. Feature extraction techniques for video processing in matlab. *Int. J. Innovative Res. Comput. Commun. Eng.*, 4: 5292-5296. DOI: 10.15680/IJIRCCE.2016.0404223

Cheolkon, J. and Q. Yang, 2016. Tingting sun, qingtao fu, hyoseob song, low light image enhancement with dual-tree complex wavelet transform. *J. Vis. Commun. Image R.*

Chien-Cheng, C., C.C. Wang and C.J. Bernard, 2014. Development of an automatic image enhancement method using singular value decomposition for visual inspection. *Int. J. Advanced Manufacturing Technol.*, 70: 679-688. DOI: 10.1007/s00170-013-5305-2

Faridul, H.S., T. Pouli, C. Chamaret, J. Stauder and E. Reinhard *et al.*, 2016. Colour Mapping: A review of recent methods, extensions and applications. *Comput. Graph. Forum*, 35: 59-88. DOI: 10.1111/cgf.12671

He Wen, W.Q. and S. Li, 2016. Medical x-ray image enhancement based on wavelet domain homomorphic filtering and clahe. *Proceedings of the International Conference Robots Intelligent System*, Aug. 27-28, IEEE Xplore Press, Zhangjiajie, China, pp: 249-254. DOI: 10.1109/ICRIS.2016.50

Honglie, X., C. Qian, Z. Chao, Y. Chunhua and L. Ning, 2015. Range limited double-thresholds multi-histogram equalization for image contrast enhancement. *Optical Rev.*, 22: 246-255. DOI: 10.1007/s10043-015-0073-x

Huang, S.C., F.C. Cheng and Y.S. Chiu, 2013. Efficient contrast enhancement using adaptive gamma correction with weighting distribution. *I. Trans. Image Proc.*, 22: 1032-1041. DOI: 10.1109/TIP.2012.2226047

Iskandarani, M.Z., 2017. Correlating and modeling of extracted features from pvt images of composites using optical flow technique and weight elimination algorithm optimization [OFT-WEA]. *J. Comput. Sci.*, 13: 371-379. DOI: 10.3844/jcssp.2017.371.379

Jing, R.T. and M.I. Nor Ashidi, 2014. Adaptive image enhancement based on bi-histogram equalization with a clipping limit. *Comput. Electrical Eng.*, 40: 86-103. DOI: 10.1016/j.compeleceng.2014.05.017

Kuldeep, S. and K. Rajiv, 2014. Image enhancement using Exposure based Sub Image Histogram Equalization. *Pattern Recognition Lett.*, 36: 10-14. DOI: 10.1016/j.patrec.2013.08.024

Kuldeep, S., R. Kapoor and K.S. Sanjeev, 2015. Enhancement of low exposure images via recursive histogram equalization algorithms. *Optik – Int. J. Light Electron Optics*, 125: 2619-2625. DOI: 10.1016/j.ijleo.2015.06.060

Liang, T., W. Ren, G. Tian, M. Elradi and Y. Gao, 2016. Low energy impact damage detection in CFRP using eddy current pulsed thermography. *Composite Structure*, 143: 352-361. DOI: 10.1016/j.compstruct.2016.02.039

Lidong, H., Z. Wei and J.W. Zebin Sun, 2015. An advanced gradient histogram and its application for contrast and gradient enhancement. *J. Visual Commun. Image Representation*, 31: 86-100. DOI: 10.1016/j.jvcir.2015.06.007

- Ma, L. and D. Liu, 2016. Delamination and fiber-bridging damage analysis of angle-ply laminates subjected to transverse loading. *J. Composit. Mat.*, 50: 3063-3075. DOI: 10.1177/0021998315615647
- Mohammad Farhan, K. and K. Ekram, Z.A. Abbasi, 2014a. Segment dependent dynamic multi-histogram equalization for image contrast enhancement. *Digital Signal Proc.*, 25: 189-223. DOI: 10.1016/j.dsp.2013.10.015
- Mohammad Farhan, K. and K. Ekram, Z.A. Abbasi, 2014b. Segment selective dynamic histogram equalization for brightness preserving contrast enhancement of images. *Optik-Int. J. Light Electron Optics*, 125: 1385-1389. DOI: 10.1016/j.ijleo.2013.08.005
- Nikolova, M. and G. Steidl, 2014. Fast hue and range preserving histogram specification: Theory and new algorithms for color image enhancement. *I. Trans. Image Proc.*, 23: 4087-4100. DOI: 10.1109/TIP.2014.2337755
- Nikolova, M., Y.W. Wen and R. Chan, 2013. Exact histogram specification for digital images using a variational approach. *J. Math. Imaging Vis.*, 46: 309-325. DOI: 10.1007%2Fs10851-012-0401-8
- Peng, G., S. Xing, X. Tan and L. Jianshu, 2015. Multi-modal medical image fusion based on the multiwavelet and nonsubsampling direction filter bank. *Int. J. Signal Proc. Image Proc. Pattern Recognition*, 8: 75-84. DOI: 10.14257/ij sip .2015.8. 11 . 0 8
- Qiong, S., Y. Wanga, K. Baia, 2016. High dynamic range infrared images detail enhancement based on local edge preserving filter. *Infrared Phys. Technol.*, 77: 464-473. DOI: 10.1016/j.infrared.2016.06.023
- Randa, A. and A.K. Rabab Farouk, 2015. Brightness preserving based on singular value decomposition for image contrast enhancement. *Optik-Int. J. Light Electron Optics*, 126: 799-803. DOI: 10.1016/j.ijleo.2015.02.025
- Santhi, K. and R.S.D. Wahida Banu, 2015. Adaptive contrast enhancement using modified histogram equalization. *Optik-Int. J. Light Electron Optics*, 126: 1809-1814. DOI: 10.1016/j.ijleo.2015.05.023
- Suganya, P., S. Gayathri and N. Mohanapriya, 2013. Survey on image enhancement techniques. *Int. J. Comput. Appli. Technol. Res.*, 2: 623-627.
- Usmantiagar, R., P. Venegas, J. Guerediaga, L. Vega and I. Lopez, 2013. Feature extraction and analysis for automatic characterization of impact damage in carbon fiber composites using active thermography. *NDT E Int.*, 54: 123-132. DOI: 10.1016/j.ndteint.2012.12.011
- Wang, F., J. Liu, Y. Liu and Y. Wang, 2016. Research on the fiber lay-up orientation detection of unidirectional CFRP laminates composite using thermal-wave radar imaging. *NDT E Int.*, 84: 54-66. DOI: 10.1016/j.ndteint.2016.08.002
- Wenda, Z., X. Zhijun, Z. Jian, Z. Fan and H. Xizhen, 2014. Variational infrared image enhancement based on adaptive dual-threshold gradient field equalization. *Infrared Phys. Technol.*, 66: 152-159. DOI: 10.1016/j.infrared.2014.05.018
- Xiangzhi, B., 2015. Morphological infrared image enhancement based on multi-scale sequential toggle operator using opening and closing as primitives. *Infrared Phys. Technol.*, 68: 143-51. DOI: 10.1016/j.infrared.2014.11.015
- Zhou, Z. and Z. Yicong, 2016. Comparative study of logarithmic image processing models for medical image enhancement. *Proceedings of the International Conference Systems Man Cybernetics*, Oct. 9-12, IEEE Xplore Press, Budapest, Hungary, pp: 001046-001050. DOI: 10.1109/SMC.2016.7844380